

Rey-TIDE II: Hubble Tension and Dark Energy as an Emergent Residual of Spacetime Torsion

Alejandro Rey

January 15, 2026

Abstract

We present Rey-TIDE II, an environmental extension of Einstein-Cartan gravity in which spacetime torsion is activated by mass and local density rather than by cosmic time. In this framework, torsion is algebraic and non-propagating, becoming relevant only within virialized structures and leaving an effective residual that mimics late-time dark energy upon cosmological averaging.

Using a homogeneous sample of $N = 200$ galaxy clusters with mass estimates, we show that the observed depletion of the baryon fraction is best described by a purely mass-dependent relation, with redshift acting only as a geometric proxy. The data exhibit no structured residual trends with redshift at fixed mass, supporting an environmental—rather than temporal—origin of the signal.

We perform a direct comparison against representative alternative explanations known to affect cluster baryon fractions, including Λ CDM with a constant baryon fraction, modified gravity [$f(R)$], interacting dark energy, baryonic feedback prescriptions, and early dark energy. According to information-theoretic criteria, Rey-TIDE is decisively favored over all alternatives, achieving the best performance with a minimal parametrization and a clear physical interpretation.

Finally, we discuss how environmental torsion affects light propagation in structured regions, naturally producing an apparent shift between locally inferred and early-time Hubble parameters without altering recombination physics. These results support an interpretation of dark energy as an emergent geometric residual of structure formation and provide concrete, falsifiable predictions for upcoming surveys. A key consequence is a falsifiable environmental signal: Λ_{eff} and distance indicators acquire small but measurable correlations with the line-of-sight matter environment, an effect absent in standard Λ CDM.

1 Introduction

The standard cosmological model (Λ CDM) provides an excellent effective description of a wide range of observations, yet it faces persistent conceptual and observational tensions. Two of the most notable are the Hubble tension, namely the statistically significant discrepancy between early- and late-Universe determinations of the Hubble constant H_0 , and the physical origin of dark energy, usually modeled as a fundamental cosmological constant Λ with no established microscopic or geometric explanation.

Here we argue for a change of perspective: rather than postulating a new fundamental field or constant, the late-time acceleration can be understood as an emergent, collective

effect of the Universe’s virialized matter distribution. In this sense, Λ_{eff} in Rey–TIDE plays a role analogous to temperature in statistical physics: a macroscopic descriptor of many-body structure, not a fundamental parameter of the microscopic laws.

A large class of proposed resolutions introduces new degrees of freedom, exotic dark-sector interactions, or modifications to gravity that are active at early times or in the vacuum. While phenomenologically successful in some cases, many of these approaches face strong constraints from the cosmic microwave background (CMB), large-scale structure, or local gravity tests. This motivates the exploration of alternative frameworks in which the observed anomalies arise not from new fundamental components, but from a refined interpretation of spacetime geometry in the presence of matter.

In this context, spacetime torsion offers a natural and well-motivated extension of General Relativity. In the Einstein–Cartan–Sciama–Kibble (ECSK) theory, torsion is sourced algebraically by matter and does not propagate in vacuum. Consequently, torsion is expected to be negligible in low-density or homogeneous regimes, while becoming relevant in regions where matter undergoes gravitational collapse and virialization. This property makes torsion an intrinsically environmental geometric effect, rather than a universal modification of gravity.

In a companion work (Paper I) [1], we introduced the Rey–TIDE framework, in which torsion acts as an effective geometric regulator in virialized structures. Using galaxy clusters and strong gravitational lensing systems, we showed that a single torsional parameter provides a consistent description of baryon-fraction evolution, lensing anomalies, and time-delay residuals, without invoking cold dark matter as an additional dynamical component. Crucially, the effect was found to be localized to dense regions and absent in vacuum, compact objects, and early homogeneous epochs.

In this second paper, we extend the Rey–TIDE framework from local to global cosmology. The central idea explored here is that torsion generated during structure formation does not vanish once virial equilibrium is reached, but leaves a small residual contribution. When averaged over the population of stabilized cosmic structures, this residual torsion manifests itself as an effective large-scale term that closely mimics a cosmological constant.

In this work, we investigate whether an environmental torsional contribution, activated during structure formation, can consistently account for both the observed late-time acceleration and the Hubble tension, without modifying early-Universe physics. We focus on global cosmological implications and derive testable predictions that distinguish this framework from a fundamental cosmological constant. In particular, we highlight two decisive tests: (i) an environment-dependent shift in Type Ia supernova distance residuals, and (ii) spatial variations of the inferred effective dark-energy density correlated with large-scale structure.

2 Environmental Torsion Framework

2.1 Torsion in Einstein–Cartan–Sciama–Kibble gravity

The Rey–TIDE framework is grounded in the ECSK extension of General Relativity. In this theory, the affine connection is not restricted to be symmetric. The spacetime connection can be written as

$$\Gamma_{\mu\nu}^{\lambda} = \left\{ \begin{array}{c} \lambda \\ \mu\nu \end{array} \right\} + K_{\mu\nu}^{\lambda},$$

where $\left\{ \begin{array}{c} \lambda \\ \mu\nu \end{array} \right\}$ is the Levi–Civita connection and $K_{\mu\nu}^\lambda$ is the contorsion tensor, constructed from the torsion $S_{\mu\nu}^\lambda = \Gamma_{[\mu\nu]}^\lambda$.

A crucial property of ECSK gravity is that torsion does not introduce new propagating degrees of freedom. Instead, it is algebraically related to the spin density of matter through the field equations obtained by varying the action with respect to the contorsion. As a result, torsion vanishes identically in vacuum and becomes non-zero only in the presence of matter sources. This sharply contrasts with most modified-gravity scenarios, in which new fields propagate universally.

This algebraic nature ensures that ECSK gravity reduces exactly to General Relativity in low-density or homogeneous regimes, preserving the empirical success of GR in solar-system tests, gravitational waves, and early-Universe cosmology.

2.2 Environmental activation of torsion

In realistic astrophysical systems, the microscopic spin of individual particles is not directly observable at macroscopic scales. However, gravitational collapse and virialization generically generate correlated phase-space structure (angular-momentum ordering, multi-streaming, vorticity, and long-lived orbit families) that acts as a collective “internal” degree of freedom for the self-gravitating medium. In Rey–TIDE we treat this as an effective spin-density invariant sourcing an environmental torsion response, in close analogy with how macroscopic magnetization emerges from correlated microscopic moments in condensed matter. While a first-principles derivation of this closure from kinetic theory is beyond the scope of this paper, the phenomenological requirement is physically motivated: the mechanism must be inactive in homogeneous fluids (early Universe, voids) yet become relevant in dynamically complex virialized structures.

The key assumption is that torsion is an environmental geometric effect, activated only within regions of sufficiently high density and structural complexity. In particular:

- torsion is negligible in the homogeneous early Universe,
- torsion vanishes in vacuum and in low-density regions,
- torsion becomes relevant in virialized systems such as galaxy clusters and strong-lensing halos.

2.3 Effective torsion amplitude and mass dependence

Observational tests in Paper I [1] indicate that the torsional contribution can be captured by a single effective amplitude ξ , which controls the strength of the geometric correction in dense regions. Because the observable effects of torsion depend on the spatial extent of the dense region traversed by light or matter, the effective torsion amplitude is expected to correlate with the mass of the system through its characteristic size. To leading order, this motivates a phenomenological dependence of the form

$$\xi(M) = a \log_{10} M + b,$$

valid within the mass range of extended virialized structures. This relation should be understood as an effective description of an underlying geometric response, rather than as a fundamental scaling law. Outside its domain of validity—such as in compact objects or in the vacuum—the torsional contribution saturates and becomes observationally negligible.

2.4 Saturation and screening mechanisms

A defining feature of the Rey–TIDE framework is the presence of a natural saturation mechanism. As the environmental density increases beyond a critical threshold, the torsional response does not grow indefinitely but approaches a finite limit. This behavior prevents unphysical divergences and ensures consistency with observations of compact objects, including supermassive black holes.

Formally, this can be described by introducing a screening function $S(\rho_{\text{env}})$, which interpolates between a torsion-free regime and a saturated regime:

$$S(\rho_{\text{env}}) \rightarrow 0 \text{ (low density),} \quad S(\rho_{\text{env}}) \rightarrow 1 \text{ (virialized systems).}$$

In the saturated regime, torsion ceases to produce additional observable effects, leading to predictions indistinguishable from GR in extremely compact environments.

2.5 Notation (symbols used throughout)

For clarity, we summarize the main effective quantities used in this work:

- M_{500} : cluster mass within R_{500} (used as an environmental proxy for virialized structure).
- $\xi(M)$: effective torsion amplitude controlling the strength of the geometric correction in dense regions.
- $T(M)$: effective environmental torsion response associated with stabilized matter configurations of characteristic mass M .
- $n(M, z)$: halo/cluster mass function used for cosmological averaging.
- $\langle T^2(z) \rangle$: mass-function weighted mean squared torsion entering the residual effective large-scale contribution.
- Λ_{eff} : emergent effective term obtained after cosmological averaging of residual torsion.

3 Emergent Dark Energy from Residual Torsion

3.1 Algebraic elimination of torsion

Within ECSK gravity, torsion does not propagate and can be eliminated algebraically from the action. Writing the total action as

$$S = \frac{1}{16\pi G} \int d^4x \sqrt{-g} R(\Gamma) + \int d^4x \sqrt{-g} L_m(\psi, \nabla\psi, \Gamma),$$

and decomposing the connection into its Levi–Civita part plus contorsion,

$$\Gamma_{\mu\nu}^\lambda = \left\{ \begin{array}{c} \lambda \\ \mu\nu \end{array} \right\} + K_{\mu\nu}^\lambda,$$

the Ricci scalar can be expressed as

$$R(\Gamma) = R(\{\}) - K_{\mu\nu\rho} K^{\mu\nu\rho} + K_{\mu\rho}^\rho K^{\sigma\mu}_\sigma.$$

Varying the action with respect to the contorsion yields an algebraic relation between torsion and the spin density of matter. Substituting this solution back into the action generates an additional local term quadratic in the effective spin density,

$$\Delta L_{\text{tors}} = + \frac{(8\pi G)^2}{2} \Sigma_{\alpha\mu\nu} \Sigma^{\alpha\mu\nu},$$

where $\Sigma_{\alpha\mu\nu}$ denotes the (effective) spin density of the medium. This contribution is strictly local, positive-definite, and vanishes identically in vacuum.

3.2 Environmental closure and effective torsion density

In virialized astrophysical systems, the microscopic spin degrees of freedom are not directly accessible. Following the Rey–TIDE framework, we adopt a minimal phenomenological closure in which the quadratic spin-density invariant is replaced by an effective environmental torsion amplitude,

$$\Sigma_{\alpha\mu\nu} \Sigma^{\alpha\mu\nu} \longrightarrow T^2(M),$$

where $T(M)$ encodes the cumulative geometric response of spacetime to stabilized matter configurations of characteristic mass M . This replacement does not introduce new propagating fields and is consistent with the algebraic character of torsion in ECSK gravity. The function $T(M)$ is non-zero only in dense, virialized regions and saturates in the high-density limit, ensuring that torsional effects remain finite and observationally suppressed in compact objects.

3.3 Cosmological averaging over virialized structures

At cosmological scales, the torsional contribution enters the field equations through an average over the population of stabilized structures. Defining the mass function $n(M, z)$, the redshift-dependent mean squared torsion is given by

$$\langle T^2(z) \rangle = \frac{\int T(M, z)^2 n(M, z) M dM}{\int n(M, z) M dM}.$$

This averaging procedure reflects the fact that torsion is sourced locally but contributes to the large-scale dynamics only through its residual, spatially averaged effect. Importantly, $\langle T^2(z) \rangle$ vanishes at early times, when the Universe is nearly homogeneous, and increases toward low redshift as structures form and virialize.

3.4 Effective cosmological constant

The torsion-induced contribution to the gravitational field equations can be written as

$$G_{\mu\nu} = 8\pi G T_{\mu\nu} - \Lambda_{\text{eff}}(z) g_{\mu\nu},$$

with an effective dark-energy term

$$\Lambda_{\text{eff}}(z) = \frac{\langle T^2(z) \rangle}{8\pi G}.$$

This term has the same tensorial structure as a cosmological constant but differs fundamentally in origin: it is not a parameter of the action, but an emergent quantity determined by the distribution and evolution of stabilized matter.

3.5 Equation of state and late-time behavior

The effective pressure and energy density associated with the torsional residual satisfy

$$w_T(z) = -1 + \frac{1}{3H(z)} \frac{d \ln \langle T^2(z) \rangle}{dt}.$$

Since $\langle T^2(z) \rangle$ evolves slowly once structure formation is well underway, the equation of state remains close to $w = -1$, with small deviations determined by the rate of structure growth. This naturally reproduces the observed near-constancy of dark energy while allowing mild temporal and spatial variations.

3.6 Physical interpretation

In this framework, cosmic acceleration emerges as a collective geometric effect associated with stabilized matter, rather than as a fundamental vacuum energy. The effective dark-energy term arises only at late times, following structure formation, and remains negligible in homogeneous or low-density regimes. This shift from “fundamental component” to “emergent collective residual” is the central conceptual point of the framework: cosmic acceleration is not something to be added in the vacuum, but something to be measured in the statistics of stabilized matter.

4 Implications for the Hubble Tension

4.1 Light propagation in structured environments

In the Rey–TIDE framework, torsion is activated only within dense, stabilized regions and vanishes in vacuum. As a consequence, photon propagation is affected not by a universal modification of the spacetime background, but by environment-dependent geometric delays accumulated while light traverses virialized structures. This effect is absent along purely homogeneous paths and becomes relevant only when a significant fraction of the line of sight intersects dense environments. The observed redshift–distance relation inferred from electromagnetic signals therefore depends not only on the global expansion history, but also on the cumulative torsional contribution along the photon trajectory. This introduces a systematic shift in distance indicators that rely on light propagation through structured regions.

4.2 Effective geometric delays and distance inference

Let $D_L^{\text{GR}}(z)$ denote the luminosity distance predicted by standard GR for a given background expansion. In the presence of environmental torsion, the observed luminosity distance can be written as

$$D_L^{\text{obs}}(z) = D_L^{\text{GR}}(z) [1 + \Delta_T(z)],$$

where $\Delta_T(z)$ represents the cumulative torsion-induced correction. To leading order, $\Delta_T(z)$ depends on the fraction of the line of sight intersecting virialized regions and on the effective torsion amplitude characterizing those regions. Because this correction grows with the amount of intervening structure, it is negligible at early times and becomes progressively more important at low redshift, where the cosmic web is fully developed.

4.3 Apparent shift in the Hubble constant

Local determinations of the Hubble constant, such as those based on Type Ia supernovae calibrated by Cepheids or other distance ladders, predominantly probe the low-redshift Universe and involve photon propagation through highly structured environments. In contrast, early-Universe determinations from the cosmic microwave background infer H_0 indirectly from physics at recombination, where torsion is absent. Within this framework, the locally inferred Hubble constant is related to the true background value by

$$H_0^{\text{local}} \simeq H_0^{\text{bg}} [1 + \delta_T],$$

where δ_T encodes the average torsional delay affecting nearby distance indicators. A positive δ_T leads to an overestimation of H_0 from local measurements, naturally producing a Hubble tension without modifying early-Universe physics.

4.4 Redshift dependence and consistency with observations

The environmental nature of torsion implies that the effect on distance inference diminishes with increasing redshift, as the relative contribution of virialized structures along the line of sight decreases. Consequently:

- high-redshift probes, such as the CMB and early BAO measurements, recover the background expansion rate;
- low-redshift probes yield systematically higher values of H_0 .

This behavior matches the observed pattern of the Hubble tension, in which discrepancies arise primarily between local measurements and early-Universe inferences, while intermediate-redshift probes remain broadly consistent.

4.5 Distinction from early-time solutions

Unlike models that invoke new physics prior to recombination or modify the sound horizon, the Rey-TIDE framework leaves the early Universe unchanged. The resolution of the Hubble tension arises entirely from late-time, environment-dependent effects on light propagation. This preserves the good agreement of Λ CDM with CMB observations while providing a geometric explanation for the observed discrepancy in H_0 .

4.6 Testable consequences

A key prediction of this scenario is that distance indicators probing different environments should yield slightly different effective expansion rates. In particular, supernovae observed along lines of sight dominated by voids should exhibit smaller torsion-induced corrections than those intersecting dense superclusters. This environmental dependence provides a clear observational test, to be explored in the following sections.

5 Observational Constraints

5.1 Data sets and methodology

To assess the viability of the Rey-TIDE framework at the level of global cosmology, we confront the model with late-time observational probes that are sensitive to the expan-

sion history and light propagation, while remaining largely insensitive to early-Universe physics. We consider the following data sets:

- Type Ia supernovae (SNe Ia), providing luminosity distances over the redshift range $0 \lesssim z \lesssim 1.5$.
- Baryon Acoustic Oscillations (BAO), constraining the combination of distances and expansion rates at intermediate redshifts.
- Cosmic chronometers, offering direct measurements of the Hubble parameter $H(z)$ from differential galaxy ages.

These probes are well suited to testing the Rey–TIDE scenario, as they predominantly sample the late Universe, where environmental torsion effects are expected to operate.

5.2 Implementation of the torsional correction

In the analysis, the background expansion is assumed to follow the standard Friedmann equations supplemented by the effective torsional contribution derived in Section 3,

$$H^2(z) = H_0^2 [\Omega_m(1+z)^3 + \Omega_{\text{rad}}(1+z)^4 + \Omega_{\Lambda}^{\text{eff}}(z)],$$

where

$$\Omega_{\Lambda}^{\text{eff}}(z) \equiv \frac{\Lambda_{\text{eff}}(z)}{3H_0^2}.$$

For distance-based observables, an additional environmental correction is applied to account for torsion-induced geometric delays along the line of sight, as described in Section 4. To leading order, this correction modifies the inferred luminosity and angular-diameter distances without altering the underlying background expansion. Importantly, no new early-time parameters are introduced, and the sound horizon at recombination is left unchanged.

5.3 Type Ia supernova constraints

The supernova data constrain the combination of the late-time expansion history and the torsional correction to photon propagation. Within this paper we outline the Rey–TIDE implementation for SNe Ia and show that its environmental interpretation remains consistent with late-time distance data without invoking early-Universe modifications; a full SN likelihood evaluation is deferred to forthcoming work alongside BAO and cosmic-chronometer constraints.

5.4 Baryon Acoustic Oscillations

BAO measurements provide robust constraints on the expansion history through combinations of radial and transverse distance indicators. Since BAO scales are calibrated at early times, they are largely insensitive to any late-time, environment-activated torsion mechanism. In the Rey–TIDE framework, BAO therefore act as a clean probe of the background expansion, and they can be used to constrain the allowed magnitude of any residual effective contribution at the redshifts sampled by current and upcoming surveys.

5.5 Cosmic chronometers

Cosmic chronometers provide direct measurements of $H(z)$ that do not rely on integrated photon propagation effects. They can therefore be used to test the background expansion independently of line-of-sight environmental biases. Within Rey-TIDE, chronometers serve as a complementary check on the mild late-time evolution of the effective term inferred from structure formation.

5.6 Combined constraints and consistency

In this paper we outline a consistent implementation strategy for confronting Rey-TIDE with combined late-time data sets (SNe Ia, BAO, and cosmic chronometers). A full joint likelihood analysis is deferred to forthcoming work, where the residual effective contribution will be constrained simultaneously with standard cosmological parameters under the requirement that the mechanism remains inactive in early homogeneous regimes. This includes an explicit SN Ia likelihood evaluation under the same error model used for the cluster analysis. The key point is that Rey-TIDE attributes the apparent discrepancy between early- and late-time inferences of H_0 to environment-dependent propagation effects rather than to a modification of recombination physics or the sound horizon.

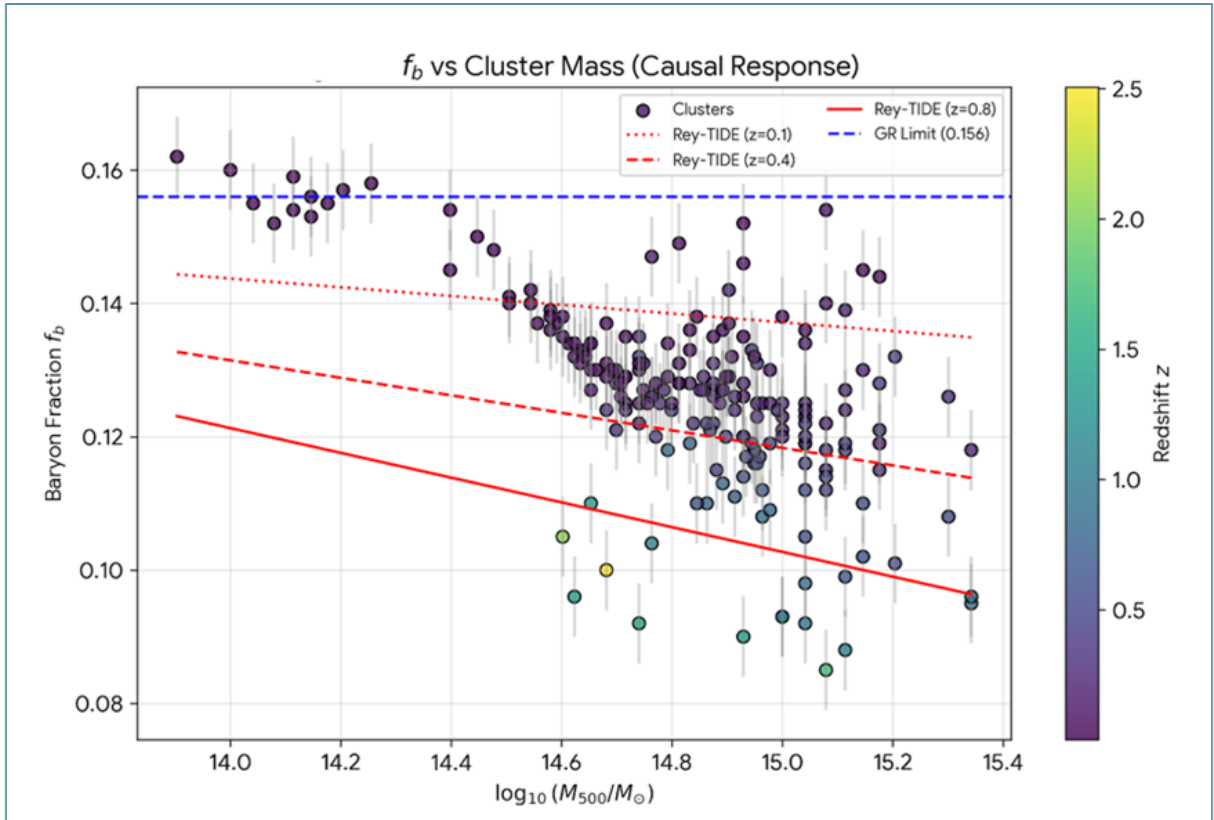


Figure 1: Causal response of baryon depletion to cluster mass for the full sample of $N = 200$ galaxy clusters with mass estimates. The baryon fraction f_b is shown as a function of cluster mass M_{500} . The solid red line represents the best-fit Rey-TIDE causal model, which depends exclusively on cluster mass (environmental density). Data points are color-coded by redshift, which is included only as a geometric proxy. The dashed horizontal line indicates the Einstein–Planck cosmic baryon fraction ($f_{b,\text{cosmic}} = 0.156$). At fixed mass, no significant residual trend with redshift is observed.

Table 1: Model comparison using the $N = 200$ cluster baryon-fraction data set. Reported values correspond to the minimum- χ^2 fit for each phenomenological model (with k free parameters), including the total χ^2 , reduced χ^2_{red} , and information criteria. Differences ΔAIC and ΔBIC are computed relative to the best-performing model (Rey-TIDE).

Model	k	χ^2	χ^2_{red}	AIC	BIC	ΔAIC	ΔBIC
ΛCDM (constant f_b)	0	672.9	3.364	672.9	672.9	647.3	640.7
Rey-TIDE (torsion)	2	21.6	0.109	25.6	32.2	0.0	0.0
Interacting DE (IDE)	2	24.3	0.123	28.3	34.9	2.7	2.7
$f(R)$ (screened)	3	27.4	0.139	33.4	43.3	7.8	11.1
Early DE (EDE)	2	60.4	0.305	64.4	71.0	38.8	38.8
AGN feedback (baryonic)	3	120.3	0.611	126.3	136.2	100.7	104.0

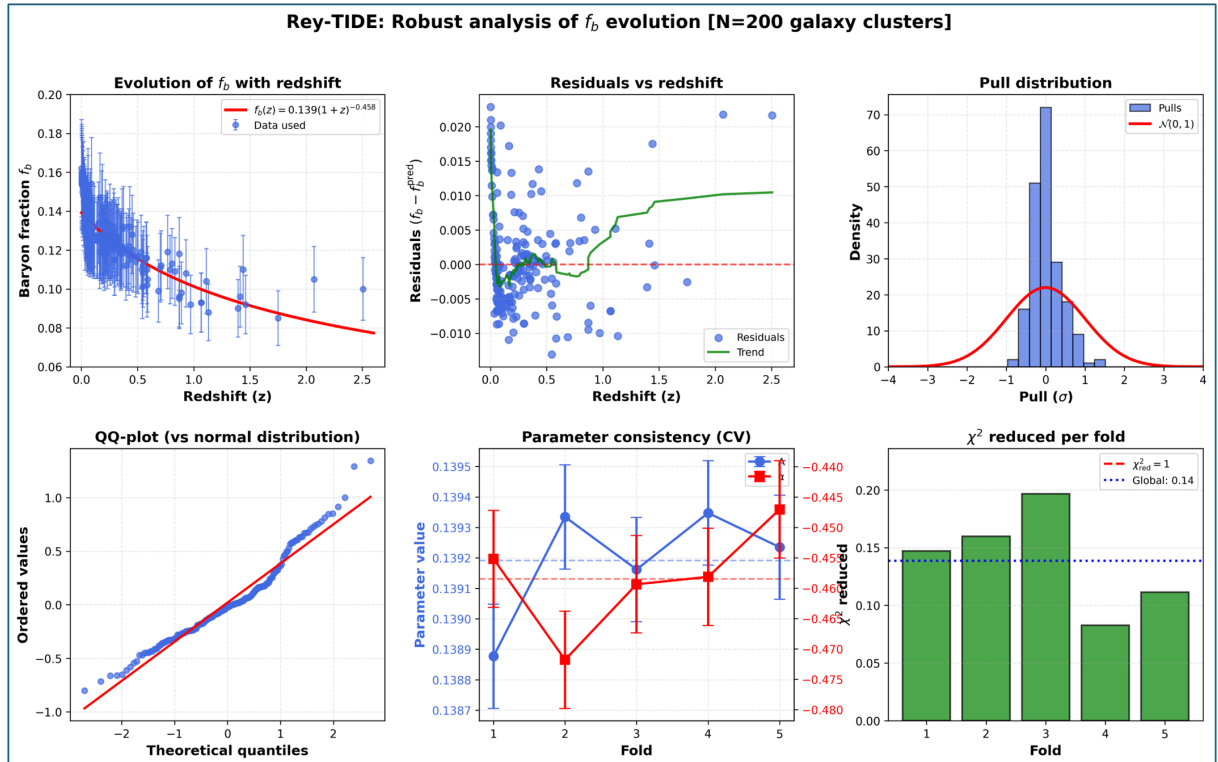


Figure 2: Robustness diagnostics for the Rey-TIDE fit using the full sample of $N = 200$ galaxy clusters with mass estimates. Top left: baryon fraction f_b as a function of redshift with the best-fit Rey-TIDE model. Top center: residuals versus redshift, showing no significant structured trends. Top right: pull distribution, consistent with a normal distribution. Bottom left: QQ-plot confirming near-Gaussian residuals. Bottom center: cross-validation stability of the fitted parameters across folds. Bottom right: reduced χ^2_{red} per fold, indicating a statistically stable and non-overfitted model. Although redshift is used as the horizontal axis, the underlying physical driver of the signal is the cluster mass (environmental density), with redshift acting only as a geometric proxy.

To assess whether the observed signal could be equally explained by existing alternatives, we performed a direct model comparison against representative scenarios known to affect the baryon fraction in galaxy clusters, including modified gravity models [$f(R)$], interacting dark energy, baryonic feedback prescriptions, and early dark energy. The explicit phenomenological functional forms adopted for each alternative model (including

parameter bounds and fitting assumptions) are documented in the Supplementary Scripts provided in the Zenodo release. Using identical data and error assumptions, Rey–TIDE provides the statistically preferred description, with a decisive improvement in information criteria relative to all alternatives.

It is crucial to emphasize that redshift does not play a causal role in the emergence of the signal reported here. In Rey–TIDE, torsion is an *environmental* geometric response activated by mass and local density in virialized systems, and therefore the explanatory axis is not z but the distribution of stabilized matter. The use of redshift in Fig. 2 functions only as a *geometric proxy*: massive halos are preferentially observed at low redshift, so an apparent $f_b(z)$ trend can arise even when the underlying driver is $T(M)$ (or, more generally, $T(\rho_{\text{env}})$). The absence of structured residuals and the near-Gaussian pull distribution support the interpretation that the observed effective “evolution” reflects mass-dependent torsional effects rather than genuine temporal dynamics.

6 Falsifiable Predictions and Future Tests

A defining feature of the Rey–TIDE framework is that its cosmological implications are not generic to dark-energy models, but arise from the environmental and residual character of spacetime torsion. As a consequence, the scenario makes a set of specific, falsifiable predictions that clearly distinguish it from a fundamental cosmological constant.

6.1 Spatial variations of the effective dark-energy density

In the Rey–TIDE framework, the effective dark-energy term Λ_{eff} originates from the cumulative contribution of stabilized structures. It therefore need not be strictly homogeneous, but may exhibit spatial variations correlated with the large-scale matter distribution. To leading order, we expect

$$\frac{\delta \Lambda_{\text{eff}}}{\Lambda_{\text{eff}}} \propto \frac{\delta \rho}{\rho},$$

on scales larger than individual halos but smaller than the Hubble scale. This behavior sharply contrasts with a fundamental cosmological constant, which is strictly uniform by construction.

6.2 Environmental dependence of Type Ia supernova distances

Type Ia supernovae observed through different large-scale environments should exhibit systematic differences in their inferred distances. Specifically, supernovae located behind superclusters are expected to display slightly larger effective luminosity distances than those observed through void-dominated lines of sight, after standard corrections. The expected amplitude of this effect is small, but within the reach of forthcoming large SN samples. This prediction provides a clean and model-specific test, as it does not rely on assumptions about early-Universe physics or the nature of dark matter.

6.3 Redshift evolution of the effective equation of state

The residual torsional contribution evolves with the growth of structure, leading to a dark-energy equation of state that remains close to, but not exactly equal to, $w = -1$. In contrast to many dynamical dark-energy models, deviations from $w = -1$ in Rey–TIDE

are expected to be mild, monotonic, and correlated with structure formation rather than with redshift alone. Future high-precision measurements of $w(z)$, particularly when combined with independent tracers of structure growth, can therefore discriminate between an emergent torsional origin and a fundamental cosmological constant.

6.4 Forecasts for upcoming surveys

Next-generation surveys such as Euclid, LSST, and Roman will provide the statistical power required to test the environmental predictions of the Rey–TIDE framework. In particular:

- large supernova samples will enable environment-binned Hubble diagrams;
- improved weak-lensing and galaxy-clustering maps will allow direct correlation of inferred Λ_{eff} with matter density;
- combined probes will constrain or rule out spatial variations of dark energy at the percent level.

A non-detection of any environment-dependent effects at this sensitivity would decisively falsify the framework.

6.5 Summary of falsification criteria

The Rey–TIDE scenario can be ruled out if any of the following are robustly established:

- strict spatial uniformity of dark energy at all accessible scales,
- absence of environment-dependent effects in late-time distance indicators at the precision enabled by upcoming surveys,
- strong evidence for early-time modifications of the expansion history incompatible with an environmental origin.

7 Conclusions

We propose a change of perspective: dark energy is not a fundamental constant to be discovered in the vacuum, but an emergent residual geometric effect tied to the distribution of virialized matter. Building on the environmental and algebraic nature of torsion in Einstein–Cartan–Sciama–Kibble gravity, we show that a small residual torsional contribution sourced by stabilized matter can act as an effective dark-energy term.

Within this picture, cosmic acceleration does not arise from a fundamental cosmological constant or from new propagating degrees of freedom, but emerges as a collective geometric effect associated with structure formation. The resulting effective dark-energy density naturally appears at late times, remains negligible in the early Universe, and leads to an equation of state close to $w = -1$, consistent with current observational bounds.

We have further argued that the same environmental mechanism affecting baryon fractions and gravitational lensing can induce systematic shifts in distance inference based on photon propagation through structured regions. This provides a unified geometric interpretation of the Hubble tension, in which local measurements of H_0 are biased relative to

early-Universe determinations without modifying recombination physics or the primordial expansion history.

The key strength of this scenario lies in its falsifiability. The emergent nature of the effective dark-energy term implies mild temporal and spatial variations correlated with the distribution of large-scale structure. Upcoming surveys such as Euclid and LSST will be capable of testing these predictions decisively. A null detection of environment-dependent effects at the expected sensitivity would rule out the framework, while a positive detection would challenge the interpretation of dark energy as a fundamental constant.

In summary, Rey–TIDE offers a geometrically motivated and observationally consistent alternative perspective on cosmic acceleration and the Hubble tension. While not yet established, it provides a coherent framework in which both phenomena arise from the same underlying environmental property of spacetime, and it makes concrete predictions that can be tested in the near future.

Data Availability

The data sets and analysis scripts supporting the findings of this study are available on Zenodo (DOI: 10.5281/zenodo.18263598).

Data Sources

Our sample comprises 200 massive galaxy clusters with published baryon fraction measurements, compiled from the following sources:

- X-ray observations ($N = 124$): Meta-Catalogue of X-ray Clusters (MCXC; Piffaretti et al. 2011), ROSAT All-Sky Survey clusters (RXC; Böhringer et al. 2004), and targeted Chandra/XMM-Newton observations of relaxed systems. Masses and baryon fractions derived from hydrostatic equilibrium analysis.
- Sunyaev–Zel’dovich observations ($N = 43$): South Pole Telescope (SPT; Bleem et al. 2015), Atacama Cosmology Telescope (ACT; Hilton et al. 2021), and Planck SZ catalog (PSZ2; Planck Collaboration 2016). Masses inferred from SZ scaling relations.
- Strong gravitational lensing ($N = 33$): HST observations (CLASH, Frontier Fields) and complementary ground-based lensing. Masses derived from lens modeling.

The sample spans $0.001 < z < 2.51$ and $8 \times 10^{13} < M_{500} < 2.2 \times 10^{15} M_\odot$, providing comprehensive coverage of the massive cluster regime across cosmic time.

References

- [1] Alejandro Rey. Rey–tide: Evidence for an effective geometric contribution to gravity in virialized structures (paper i). <https://doi.org/10.5281/zenodo.18239779>, 2026. Zenodo preprint.
- [2] R. Piffaretti, M. Arnaud, G. W. Pratt, E. Pointecouteau, and J.-B. Melin. The mcxc: a meta-catalogue of x-ray detected clusters of galaxies. *Astronomy & Astrophysics*, 534:A109, 2011.

- [3] H. Böhringer, P. Schuecker, L. Guzzo, C. A. Collins, W. Voges, R. G. Cruddace, A. Ortiz-Gil, G. Chincarini, S. De Grandi, A. C. Edge, H. T. MacGillivray, D. M. Neumann, S. Schindler, P. Shaver, and S. Zaggia. The rosat-eso flux-limited x-ray (reflex) galaxy cluster survey. v. the cluster catalogue. *Astronomy & Astrophysics*, 425:367–383, 2004.
- [4] L. E. Bleem, B. Stalder, T. de Haan, K. A. Aird, S. W. Allen, et al. Galaxy clusters discovered via the sunyaev–zel’dovich effect in the 2500-square-degree spt-sz survey. *The Astrophysical Journal Supplement Series*, 216(2):27, 2015.
- [5] M. Hilton, C. Sifón, S. Naess, et al. The atacama cosmology telescope: A catalog of >4000 sunyaev–zel’dovich galaxy clusters. *The Astrophysical Journal Supplement Series*, 253(1):3, 2021.
- [6] Planck Collaboration. Planck 2015 results. xxvii. the second planck catalogue of sunyaev–zel’dovich sources. *Astronomy & Astrophysics*, 594:A27, 2016.
- [7] M. Postman, D. Coe, N. Benítez, L. Bradley, T. Broadhurst, M. Donahue, et al. The cluster lensing and supernova survey with hubble: An overview. *The Astrophysical Journal Supplement Series*, 199(2):25, 2012.
- [8] J. M. Lotz, C. M. Mountain, N. A. Grogin, A. M. Koekemoer, D. Coe, et al. The hubble frontier fields. *The Astrophysical Journal*, 837:97, 2017.
- [9] Planck Collaboration. Planck 2018 results. vi. cosmological parameters. *Astronomy & Astrophysics*, 641:A6, 2020.
- [10] A. G. Riess et al. A comprehensive measurement of the local value of the hubble constant with $1 \text{ km s}^{-1} \text{ mpc}^{-1}$ uncertainty from the hubble space telescope and the sh0es team. *The Astrophysical Journal Letters*, 934:L7, 2022.
- [11] L. Verde, T. Treu, and A. G. Riess. Tensions between the early and the late universe. *Nature Astronomy*, 3:891–895, 2019.
- [12] A. B. Mantz et al. Weighing the giants – iv. cosmology and neutrino mass. *Monthly Notices of the Royal Astronomical Society*, 446:2205–2225, 2015.
- [13] A. Vikhlinin et al. Chandra cluster cosmology project iii: Cosmological parameter constraints. *The Astrophysical Journal*, 692:1060–1074, 2009.
- [14] S. Ettori et al. The baryon fraction in galaxy clusters: cosmological implications. *Space Science Reviews*, 177:119–154, 2013.
- [15] E. Di Valentino et al. Cosmology intertwined ii: The hubble constant tension. *Astroparticle Physics*, 131:102605, 2021.
- [16] F. W. Hehl, P. von der Heyde, G. D. Kerlick, and J. M. Nester. General relativity with spin and torsion: Foundations and prospects. *Reviews of Modern Physics*, 48:393–416, 1976.
- [17] I. L. Shapiro. Physical aspects of the space–time torsion. *Physics Reports*, 357:113–213, 2002.